COMMUNICATIONS IN SCIENCE AND TECHNOLOGY

Homepage: cst.kipmi.or.id

Mission-level energy efficiency optimization for multi-UAV data collection using a genetic algorithm

Muhammad Anif[a,b], Selo Sulistyo[a,*], I Wayan Mustika[a]

[a]*Department of Electrical and Information Engineering, Universitas Gadjah Mada, Yogyakarta 55281, Indonesia*
[b]*Department of Electrical Engineering, Politeknik Negeri Semarang, Semarang 50275, Indonesia*

Article history:
Received: 21 January 2026 / Received in revised form: 15 April 2026 / Accepted: 22 April 2026

Abstract

The efficient utilization of limited onboard energy remains a fundamental challenge in cooperative multi-UAV data collection missions. Existing routing approaches typically optimize surrogate objectives, such as travel distance or aggregate energy consumption, which do not directly reflect mission effectiveness. The present paper proposes a Mission-level Energy-aware Genetic Algorithm (ME-GA) that directly maximizes mission-level energy efficiency, defined as the ratio of successfully delivered sensing data to total energy consumption. The proposed framework integrates a mission-level simulator into the fitness evaluation, explicitly modeling UAV propulsion, sensing, data buffering, wireless communication, and return-to-base feasibility under energy constraints. Extensive simulations involving up to 9 UAVs and 100 Points of Interest (PoIs) under both grid and random spatial layouts demonstrate that ME-GA consistently achieves high and stable energy efficiency while maintaining near-complete task satisfaction and high data delivery reliability. In comparison to GA-based baselines, the proposed approach enhances energy efficiency by approximately 5–15% across the evaluated scenarios along with a reduction in total travel distance by up to 40% in larger fleet sizes. Overall, the results demonstrate that mission-level energy efficiency serves as a unified and physically meaningful objective for multi-UAV optimization, enabling robust and scalable performance across diverse operational scenarios.

Keywords: Multi-UAV systems; genetic algorithm; mission-level optimization; energy efficiency; data collection

1. Introduction

The utilization of multiple Unmanned Aerial Vehicles (UAVs) for cooperative data collection has emerged as a promising paradigm for efficient sensing in large-scale and hard-to-reach environments, including environmental monitoring, smart agriculture, disaster response, photogrammetry, and surveillance applications [1–5]. In a standard mission, a fleet of UAVs is deployed from a Base Station (BS) to visit spatially distributed Points of Interest (PoIs), perform sensing tasks, and transmit the collected data back to the BS. Despite their operational flexibility, UAVs – particularly rotary-wing platforms– are fundamentally constrained by limited onboard energy, which restricts mission duration, spatial coverage, and data delivery capability [6].

To address these challenges, there has been extensive research conducted on UAV path planning and communication-aware optimization. It is evident that these problems are generally NP-hard in nature, as they extend classical combinatorial formulations such as the Traveling Salesman Problem (TSP) and the Vehicle Routing Problem (VRP) by incorporating energy constraints, communication requirements, and mission feasibility considerations [7–9]. Consequently, exact optimization methods become computationally intractable for realistic scenarios, thus motivating the adoption of heuristic and metaheuristic approaches.

Early approaches were predominantly reliant upon greedy heuristics, a consequence of their simplicity and minimal computational cost. For instance, nearest-neighbor strategies construct UAV routes incrementally based on local criteria such as distance or energy consumption [10]. However, such methods frequently exhibit suboptimal performance and restricted scalability as the problem size increases.

To enhance the quality of solutions, population-based metaheuristic algorithms such as Particle Swarm Optimization (PSO) and Ant Colony Optimization (ACO) have been employed in the context of multi-UAV routing problems [11,12]. These methods leverage collective search mechanisms to explore large solution spaces more effectively. Nevertheless, they typically optimize simplified surrogate objectives, such as travel distance or aggregate energy consumption, which do not directly reflect mission effectiveness.

* Corresponding author.
Email: selo@ugm.ac.id
https://doi.org/10.21924/cst.11.1.2026.1901

In parallel, communication-aware trajectory optimization has garnered increasing attention, emphasizing the interdependence between UAV mobility and wireless communication performance [13,14]. While these studies have highlighted the significance of link quality and data transmission, most formulations continue to prioritize intermediate metrics such as throughput or connectivity, rather than end-to-end mission outcomes.

Genetic Algorithm (GA)-based approaches have also been extensively adopted due to their flexibility in handling combinatorial optimization problems involving routing and task allocation [15–17]. Subsequent studies incorporated energy-aware constraints and load-balancing strategies to improve the feasibility and fairness of the system among UAVs [18,19]. However, similar to other metaheuristic methods, these approaches generally optimize surrogate objectives (e.g., distance or total energy), which may not accurately capture the ultimate mission goal.

Multi-objective evolutionary algorithms, such as the Nondominated Sorting Genetic Algorithm II (NSGA-II), further extend this framework by jointly optimizing multiple conflicting objectives, including energy consumption, coverage, and communication performance [20,21]. Although such approaches provide flexibility in exploring trade-offs, they necessitate post hoc decision-making to select a single deployable solution, a process which may reduce interpretability and complicate practical deployment.

More recently, deep reinforcement learning (DRL)-based methods have been explored with a view to enabling adaptive decision-making in dynamic environments [22,23]. While these approaches are capable of learning complex policies and handling uncertainty, they typically necessitate substantial training data, high computational resources, and frequently lack interpretability in comparison to classical optimization methods.

Despite significant advances in the field, a fundamental limitation persists across existing studies: the optimization objective is rarely aligned with the true mission goal. Most approaches focus on minimizing energy consumption, travel distance, or maximizing intermediate communication metrics, while treating mission effectiveness –particularly the amount of successfully delivered sensing data– as a secondary evaluation criterion [24,25].

From a mission-centric perspective, the primary objective of an energy-constrained multi-UAV data collection mission is not merely to minimize energy consumption or travel distance, but to maximize the amount of useful sensing data delivered per unit of energy consumed. This concept, referred to as mission-level energy efficiency, provides a physically meaningful and operationally relevant performance metric. However, it is rarely adopted as a direct optimization objective and is typically utilized used solely for post hoc evaluation.

In response to this identified gap, this paper proposes a Mission-level Energy-aware Genetic Algorithm (ME-GA) that directly maximizes mission-level energy efficiency. The proposed approach integrates a mission-level simulator into the fitness evaluation, explicitly modeling UAV propulsion, sensing, data buffering, wireless communication, and return-to-base feasibility under energy constraints. The proposed framework ensures that the search process is directly aligned with mission outcomes by embedding end-to-end mission dynamics within the optimization loop.

The contributions of this work are threefold. Firstly, mission-level energy efficiency is formulated as the primary optimization objective for multi-UAV data collection. Secondly, we have developed ME-GA, a genetic algorithm framework that integrates mission-level simulation into the fitness evaluation. Thirdly, extensive simulations have been conducted with statistical analysis to validate the performance of the proposed approach against baseline methods, including Random, Greedy, MR-GA, EB-GA, and NSGA-II across diverse operational scenarios.

2. Materials and Methods

2.1. System model

This study considers a cooperative multi-UAV data collection mission conducted over a two-dimensional area of 1000×1000 m. Within this region, a fleet of M rotary-wing UAVs, denoted by $\mathcal{U} = \{1, 2, \ldots, M\}$, is deployed from a central Base Station (BS), which also serves as the data sink. A set of N Points of Interest (PoIs) that are distributed over specific area, denoted by $\mathcal{P} = \{1, 2, \ldots, N\}$, is predefined within the designated mission area, as illustrated in Fig. 1.

To ensure both controlled evaluation and realistic validation, two PoI distribution scenarios are considered: (i) a grid-based layout for structured analysis and reproducibility, and (ii) a random layout to represent irregular real-world deployments.

Each Point of Interest (PoI) is associated with a sensing data demand that must be collected and delivered to the BS. It is imperative that each PoI is constrained to be visited at most once, thereby ensuring that redundant sensing is avoided. In the event that a given PoI is not visited within the designated mission duration, it is considered to be unserved. This then will result in a failure to contribute to mission performance.

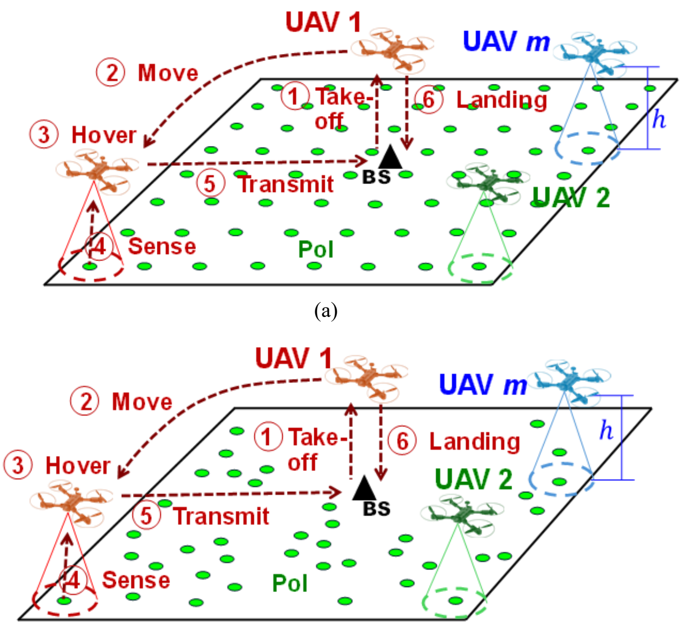

(b)

Fig. 1. Multi-UAV data collection system model: (a) grid PoI layout, and (b) random PoI layout

The system employs a centralized offline mission planning framework, in which UAV routes are optimized prior to deployment. During execution, UAVs operate autonomously without inter-UAV communication. The term "cooperative" refers to joint mission planning rather than real-time coordination.

Each UAV follows a trajectory that starts and ends at the BS, visiting a subset of PoIs. The mission evolves over discrete timeslots, during which UAVs may perform movement, sensing, or data transmission.

2.2. Data collection and delivery model

Each PoI $n \in \mathcal{P}$ has an initial data demand D_n^{req}. During mission execution, UAVs collect data from PoIs based on sensing duration and rate. The total data collected by UAV *m* is

$$D_m^{\text{col}} = \sum_{n \in \mathcal{P}} D_{m,n}^{\text{col}}. \tag{1}$$

The collected data are temporarily stored in the UAV's onboard buffer and transmitted to the BS via an uplink wireless channel. The total data delivered is then given by

$$D^{\text{tot}} = \sum_{m=1}^{M} D_m^{\text{del}}. \tag{2}$$

Only data successfully received at the BS contribute to mission performance. Data remaining in UAV buffers or lost due to mission termination are considered undelivered.

2.3. Communication model

The uplink communication between UAVs and the BS is modeled utilizing an air-to-ground channel model that incorporates large-scale and small-scale effects [26].

The received signal is contingent upon distance-independent path loss and probabilistic Line-of-Sight (LoS) conditions, encompassing free-space path loss, additional attenuation for Non-Line-of-Sight (NLoS), and log-normal shadowing [27]. The probability of LoS is modeled as a function of elevation angle utilizing a logistic function [28].

Small-scale fading is modeled as Rician fading under LoS conditions, and Rayleigh fading under NLoS conditions. This model captures realistic fluctuations in the channel in view of multipath propagation.

The instantaneous SINR is computed as follows:

$$\gamma_m = \frac{P^{\text{tx}} \cdot G^{\text{tx}} \cdot G^{\text{rx}} \cdot F_m \cdot 10^{-PL_{m,sh}/10}}{P^{\text{noise}} + I_m} \tag{3}$$

where P^{tx} represents UAV transmit power, G^{tx} and G^{rx} denote the linear antenna gains of UAV and the BS, respectively. F_m is the small-scale fading, and $PL_{m,sh}$ is the large-scale path loss including shadowing and NLoS loss (expressed in dB). P^{noise} is defined as the total receiver noise power over the communication bandwidth, and I_m is defined as the aggregate interference power.

The achievable uplink rate is determined using a modulation and coding scheme (MCS)-based mapping, which converts SINR values into discrete spectral efficiency levels [29]. The resulting data rate is

$$\rho_m^{\text{com}} = \eta^{\text{MAC}} \cdot \eta^{\text{MCS}}(\gamma_m) \cdot B_w \tag{4}$$

where η^{MAC} accounts for protocol overhead, $\eta^{\text{MCS}}(\gamma_m)$ is the spectral efficiency of the MCS table, and B_w is the communication bandwidth. This approach captures realistic communication behavior, including discrete rate adaptation and physical-layer constraints, in contrast to simplified constant-rate models.

It is assumed that a communication link is available when a UAV is within communication range. The model does not explicitly account for multi-user interference or resource contention. This abstraction represents a best-case communication scenario and is adopted to isolate the impact of routing decisions and ensure tractable simulation complexity. These models are consistent with recent communication-aware UAV studies that incorporate realistic channel conditions and adaptive rate control mechanisms [30].

2.4. Energy consumption model

The total energy consumption of each UAV accounts for multiple operational components. For UAV *m*, the total energy consumption is expressed as follows:

$$E_m^{\text{tot}} = E_m^{\text{to}} + E_m^{\text{mv}} + E_m^{\text{sn}} + E_m^{\text{tx}} + E_m^{\text{hv}} + E_m^{\text{ld}}, \tag{5}$$

where the components in question correspond to the following functions: take-off, horizontal movement, sensing, data transmission, hovering, and landing. Each component is modeled as the product of a constant power coefficient and its corresponding operation duration [31,32]. This formulation provides a unified representation of heterogeneous energy expenditures across different mission phases.

The mission-level total energy consumption is given by

$$E^{\text{tot}} = \sum_{m=1}^{M} E_m^{\text{tot}}. \tag{6}$$

The mission is considered feasible on the condition that the energy consumption of each UAV does not exceed its initial onboard energy capacity

$$E_m^{\text{tot}} \le E_m^{\text{init}}, \qquad \forall m \in \mathcal{U}. \tag{7}$$

The UAV motion model employs a constant-velocity kinematic abstraction, which disregards acceleration, deceleration, and maneuvering dynamics. This abstraction is appropriate for mission-level planning, where average energy consumption dominates total energy expenditure. It is therefore considered that transient effects such as acceleration and turning are negligible at the planning level. Despite its simplification, this model has gained widespread adoption in mission-level UAV studies, and providing a reasonable approximation for long-duration operations [33–35].

All UAVs are required to complete their assigned routes, ensuring the transmission of collected data, and a timely return to the BS without exceeding their energy limits. UAVs that violate this constraint are considered to be infeasible and are terminated during the simulation. The execution of mission is simulated over a finite time horizon, with the discrete time slots. At each timeslot, UAV states including positions, sensing activity, buffer occupancy, energy consumption, and data transmission are updated. The simulation is terminated by the delivery of all data, or by the inactivity of UAVs. This timeslot-based simulation facilitates consistent evaluation of complex interactions between motion, sensing, and communication.

2.5. Mission-level energy efficiency metric

The primary performance metric, i.e., mission-level energy efficiency, is defined as the ratio between the total amount of data delivered and the total energy consumed as follows:

$$\eta = \frac{D^{\text{tot}}}{E^{\text{tot}}}. \tag{8}$$

This metric directly quantifies the efficiency with which energy is converted into useful mission output. In contrast to surrogate objectives, it captures end-to-end system performance.

2.6. Problem formulation

The objective is to determine a set of UAV routes $\mathcal{R} = \{\mathcal{R}_1, ..., \mathcal{R}_M\}$ that maximize mission-level energy efficiency while satisfying energy and feasibility constraints. The optimization problem can be expressed in the following form:

$$(P1): \max_{\mathcal{R}} \eta \tag{9}$$

s.t. $E_m^{\text{tot}} \le E_m^{\text{init}},\ \forall m,$

$\mathcal{R}_m \cap \mathcal{R}_{m'} = \emptyset,$

$\bigcup_{m=1}^{M} \mathcal{R}_m \subseteq \mathcal{P},$

each UAV route starts and ends at the BS,

each PoI is visited at most once.

This problem is combinatorial in nature and NP-hard, which in turn motivates the use of metaheuristic optimization methods. Table 1 provides a summary of the primary parameters and constant values employed in data and energy models [36] during the course of the experiments. It is imperative to note that these parameters are kept constant across all algorithms to ensure fair comparison.

2.7. Mission-level energy-aware genetic algorithm (ME-GA)

The present study proposes a Mission-level Energy-aware Genetic Algorithm (ME-GA) to solve the formulated optimization problem. Fig. 2 provides a synopsis of the overall workflow of the proposed ME-GA framework.

The process begins with chromosome encoding utilizing a permutation vector and a cut vector, subsequently followed by route decoding into multi-UAV trajectories. The evaluation of these routes is conducted through the utilization of a mission-level simulator, which computes the mission-level energy efficiency and assigns it a fitness value. The evolutionary process is characterized by the iterative updating of the population through selection, crossover, and mutation until convergence is achieved.

Table 1. Simulation parameters employed in data and energy model

Parameter	Notation	Value
Number of PoIs	N	100
Number of UAVs	M	1–9
PoI data demand	D_n^{req}	5 MB
UAV initial/threshold energy	E_m^{init} / E_m^{th}	343 / 17 kJ
UAV flight altitude	h	50 m
UAV take-off / propulsion / landing velocity	v^{to} / v^{hz} / v^{ld}	5 / 10 / 3 m/s
UAV take-off / propulsion / sensing / transmitting / hovering / landing power	P^{to} / P^{mv} / P^{sn} / P^{tx} / P^{hv} / P^{ld}	179 / 114 / 15 / 5 / 127 / 115 W
Sensing range / sensing data rate	r^{sn} / ρ^{sn}	50.1 m / 0.4 Mbps
Carrier frequency / bandwidth / noise power	f_c / B_w / P^{noise}	2.4 GHz / 20 MHz / -90 dBm
Timeslot duration / time horizon	Δt / T	1 s / 3000 timeslots

Each candidate solution represents a complete cooperative mission plan, encoded as a chromosome that jointly captures both the PoI visiting order and the task partitioning among multiple UAVs. This unified representation facilitates simultaneous optimization of routing structure and workload allocation within a single evolutionary framework.

Formally, a chromosome is defined as

$$C = (\boldsymbol{\pi}, \boldsymbol{\kappa}), \tag{10}$$

where $\boldsymbol{\pi}$ is a permutation vector of length N that specifies a global visiting order of all PoIs, and $\boldsymbol{\kappa}$ is a cut vector that divides this permutation into M segments assigned to a single UAVs. The permutation vector

$$\boldsymbol{\pi} = (\pi_1, \pi_2, \dots, \pi_N), \tag{11}$$

is a bijection over the PoI index set $\mathcal{P}$, ensuring that each PoI is visited at most once during the mission. The cut vector

$$\boldsymbol{\kappa} = (\kappa_1, \kappa_2, \dots, \kappa_{M-1}), \tag{12}$$

defines M disjoint subsequences of $\boldsymbol{\pi}$, where κ_m indicates the boundary between the PoI subsequences assigned to UAV m and UAV $m + 1$.

During the process of decoding, the chromosome C is transformed into an explicit multi-UAV route set

$$\mathcal{R} = \{\mathcal{R}_1, \mathcal{R}_2, \dots, \mathcal{R}_M\}, \tag{13}$$

where each route $\mathcal{R}_m$ consists of a subsequence of PoIs derived from $\boldsymbol{\pi}$ according to $\boldsymbol{\kappa}$, with the BS implicitly prepended and appended. This decoding process guarantees route feasibility in terms of PoI uniqueness while allowing flexible workload distribution across UAVs. A two-part chromosome structure of this kind is particularly well suited to cooperative multi-UAV missions, as it decouples the global visitation order from UAV-level assignment. This facilitates the effective exploration of both routing and load-balancing dimensions by genetic operators.

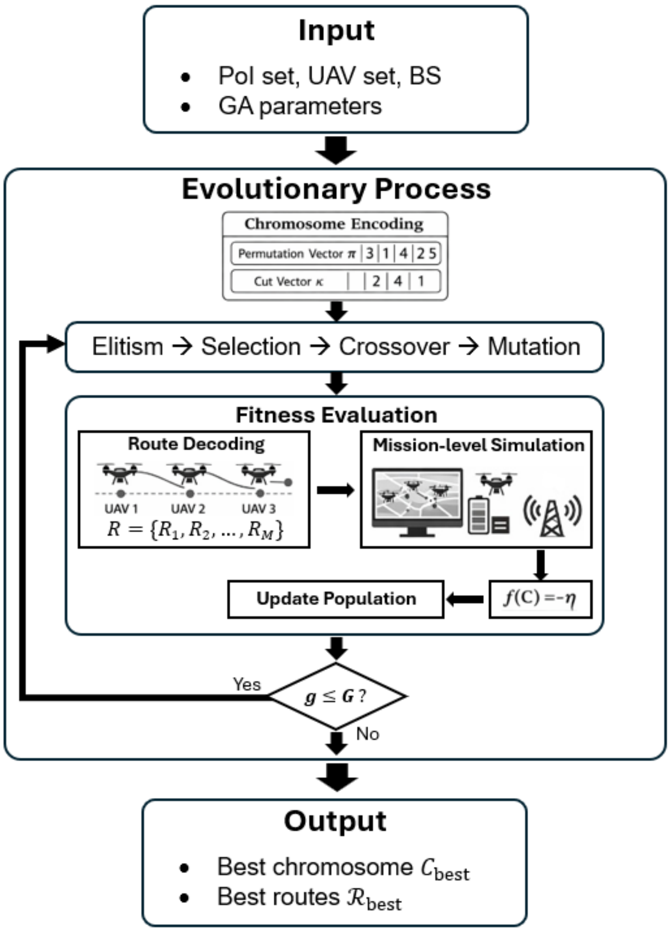

Fig. 2. Overall methodology of the proposed ME-GA framework

The evolutionary search process in ME-GA is governed by a set of standard genetic algorithm parameters that control population diversity, selection pressure, and convergence behavior. The initial population is generated using a hybrid initialization strategy that combines heuristic-based solutions with randomly generated chromosomes, thereby ensuring baseline feasibility while preserving population diversity. Key parameters, including population size, number of generations, tournament size, elitism rate, crossover rate, and mutation rate, are kept fixed across all GA-based algorithms considered in this study to ensure a fair and reproducible evaluation. Table 2 summarizes the parameter settings utilized in all experiments, which were selected through preliminary tuning to achieve a balance between solution quality and computational cost.

In contrast to conventional GA-based approaches, ME-GA does not rely on surrogate or proxy fitness functions. Instead, each chromosome is evaluated using a mission-level simulator. Given a candidate chromosome, the simulator executes the corresponding multi-UAV mission while explicitly modeling UAV propulsion, sensing operations, onboard data buffering, wireless communication, and return-to-base feasibility under energy constraints. The resulting mission-level energy efficiency, denoted by η, is employed directly as the fitness measure, thereby aligning the evolutionary search with physically meaningful and end-to-end mission outcomes.

Table 2. GA parameters utilized in experiments

Parameter	Notation	Value
Population size / number of generations / tournament size	N_{pop} / G / τ	50 / 100 / 3
Elitism rate / crossover rate / mutation rate	ρ_{ε} / ρ_{c} / ρ_{m}	0.1 / 0.9 / 0.1

Upon the basis of this fitness evaluation, standard genetic operators — including selection, crossover, and mutation — are iteratively applied to evolve the population in the direction of solutions with higher mission-level energy efficiency. Chromosomes that violate energy constraints or fail to ensure feasible return-to-base trajectories are penalized or discarded during fitness evaluation, ensuring that only operationally viable solutions are propagated. The evolutionary process is terminated after a predetermined number of generations or upon convergence, and the chromosome that maximizes mission-level energy efficiency is selected as the final solution.

In addition, elitism rate ensures that a fraction of the best-performing chromosomes is preserved across generations, thereby preventing loss of high-quality solutions due to stochastic variation. The crossover rate controls the frequency at which route structures undergo recombination through order crossover on the permutation vector. Conversely, the mutation rate introduces stochastic perturbations to both the permutation and cut vectors, in so doing, maintaining population diversity and mitigating premature convergence.

Algorithm 1 presents the overall evolutionary framework of ME-GA, including population initialization, genetic operators, and solution selection. The present framework has been intentionally designed to be independent of the specific optimization objective. The evaluation of candidate solutions is delegated to Algorithm 2, which defines the mission-level objective and fitness computation. It is notable that during both population initialization and offspring generation stages, Algorithm 1 repeatedly invokes Algorithm 2 to evaluate chromosomes. The modular design of the system enables the optimization of different mission objectives within the same evolutionary framework by modifying only the evaluation procedure, while the genetic operators and control flow remain unaltered.

Algorithm 1 outlines the overall workflow of ME-GA for cooperative multi-UAV data collection. The algorithm requires as inputs the set of PoI with associated data demands, the UAV fleet with initial energy budgets, the location of the BS, and standard GA parameters. The procedure begins with the construction of an initial population through a hybrid initialization strategy that integrates heuristic-based and random chromosomes. This ensures both feasibility and diversity (Line 1). Each chromosome in the initial population is then evaluated using the mission-level fitness evaluation defined in Algorithm 2 (Line 2), after which the generation counter is initialized (Line 3).

The evolutionary process is characterized by its iterative nature, whereby it continues until the maximum number of generations is attained (Line 4). At each generation, a subset of elite chromosomes is preserved according to the elitism rate, denoted by $\rho_{\mathcal{E}}$, thus preventing the loss of high-quality solutions (Line 5). These elite individuals are directly copied into the next generation (Line 6).

The remaining population is generated through standard GA operators. The parent chromosomes are selected from the current population using tournament selection process, with tournament size τ (Line 8). The order crossover method is applied to the permutation vector $\boldsymbol{\pi}$ with probability ρ_c, thereby allowing route structures to be exchanged while preserving feasible PoI ordering (Line 9). Mutation is then applied to both the permutation vector $\boldsymbol{\pi}$ and the cut vector $\boldsymbol{\kappa}$ with probability ρ_m, thus enabling local perturbations in route assignment and UAV workload distribution (Line 10).

Each offspring chromosome is evaluated using Algorithm 2 (Line 11) and subsequently inserted into the next-generation population until the predefined population size is reached (Lines 7–12). The generation index is then incremented, and the evolutionary loop continues (Line 13).

Algorithm 1. ME-GA Framework

Input:
PoI set $\mathcal{P} = \{1, \dots, N\}$ with data demand D_n^{req}
UAV set $\mathcal{U} = \{1, \dots, M\}$ with initial energy E_m^{init}
Base Station location BS
GA parameters: Population size N_{pop}, Number of generations G, Tournament size τ, Elitism rate $\rho_{\mathcal{E}}$, Crossover rate ρ_{c}, Mutation rate ρ_{m}
Output:
Best chromosome C_{best}
Decoded multi-UAV routes $\mathcal{R}_{\text{best}}$

1: Initialize population $\mathcal{X}^{(0)}$ using hybrid initialization
2: Evaluate each chromosome $C \in \mathcal{X}^{(0)}$ utilizing Algorithm 2 to obtain fitness function $f(C)$
3: Set generation index $g \leftarrow 0$
4: **While** $g < G$ **do**
5: Select elite chromosomes from $\mathcal{X}^{(g)}$ according to $\rho_{\mathcal{E}}$
6: Initialize $\mathcal{X}^{(g+1)}$ with elite chromosomes
7: **While** $|\mathcal{X}^{(g+1)}| < N_{pop}$ **do**
8: Select parent chromosomes from $\mathcal{X}^{(g)}$ utilizing tournament selection (τ)
9: Apply order crossover on $\boldsymbol{\pi}$ with probability ρ_c
10: Apply mutation on $\boldsymbol{\pi}$ and $\boldsymbol{\kappa}$ with probability ρ_m
11: Evaluate offspring utilizing Algorithm 2
12: Insert offspring into $\mathcal{X}^{(g+1)}$
13: Set $g \leftarrow g + 1$
14: Select $C_{\text{best}} = \arg\min_{C \in \mathcal{X}^{(G)}} f(C)$
15: Decode C_{best} into UAV route set $\mathcal{R}_{\text{best}}$
16: Return $C_{\text{best}}, \mathcal{R}_{\text{best}}$

Following the completion of all generations, the chromosome with the minimum fitness value –corresponding to the maximum mission-level energy efficiency– is selected as the final solution (Line 14). This best chromosome is then decoded into a set of explicit multi-UAV routes for mission execution (Line 15), and both the chromosome and its decoded routes are returned as the algorithm output (Line 16).

Algorithm 2 defines the mission-level objective and fitness evaluation procedure employed by ME-GA. In the context of a chromosome $C = (\boldsymbol{\pi}, \boldsymbol{\kappa})$ and common initial mission state $\mathbf{s}_0$, the chromosome is first decoded into a set of cooperative multi-UAV routes $\mathcal{R}$ (Line 1). To ensure fair and consistent comparison among candidate solutions, the simulator is initialized to the same initial state $\mathbf{s}_0$ for every fitness evaluation (Line 2). The decoded routes are then executed within a mission-level simulator, represented by the simulation operator $\Phi(\cdot)$, which explicitly models UAV propulsion, sensing, data buffering, wireless communication, and return-to-base feasibility (Line 3). The simulator produces mission outcome metrics, including the total amount of data successfully delivered to the base station and the total energy consumed by all UAVs.

Based on these mission outcomes, the mission-level energy efficiency, denoted by the symbol η, is calculated as the ratio between the total volume of delivered data and the total energy expenditure (see Line 4). The fitness value is finally defined as the negative of the efficiency metric as follows:

$$f(C) = -\eta. \tag{14}$$

This directly corresponds to maximization of mission-level energy efficiency in the GA minimization process (Line 5).

Algorithm 2. Objective and fitness evaluation for ME-GA

Input:
Chromosome $C = (\boldsymbol{\pi}, \boldsymbol{\kappa})$, initial state $\mathbf{s}_0$
Output:
Fitness value $f(C)$

1: Decode chromosome C into multi-UAV routes $\mathcal{R}$
2: Initialize simulator state to $\mathbf{s}_0$
3: Run mission-level simulation $\mathcal{K} \leftarrow \Phi(\mathcal{R}, \mathbf{s}_0)$
4: Compute mission-level energy efficiency η
5: Return fitness value $f(C) = -\eta$

2.8. Benchmark algorithms

ME-GA is compared against a selection of five baseline algorithms within the context of identical environment parameters, time-slot simulation settings, and UAV energy constraints.

- **Random assignment:** Points of interest (PoIs) are randomly assigned and randomly ordered for each UAV. This baseline provides a minimum threshold for structured planning performance, thereby emphasizing the benefit of guided optimization [37].
- **Greedy (nearest-neighbor):** Each UAV then iteratively selects the next unvisited PoI based on the minimum incremental travel distance (or local movement cost), after which it returns to the BS when its energy is insufficient to continue. Greedy is computationally lightweight and often competitive in small instances, but it may suffer from local myopia and reduced coverage/data delivery in larger missions [38].
- **Multi-Route Genetic Algorithm (MR-GA):** The GA

baseline optimizes route structure primarily through the utilization of distance/energy surrogate objectives (e.g., shorter routes and feasibility), without the explicit maximization of delivered-data-per-energy [39]. It is the representation of conventional evolutionary routing extensions of TSP/VRP-style formulations.

- **Energy-Balanced Genetic Algorithm (EB-GA):** A GA variant penalizes imbalance in the energy consumptions of Unmanned Aerial Vehicles (UAV) to avoid early depletion of a subset of UAVs. While enhancing robustness, its target remains energy-centric and does not directly quantify mission productivity per unit energy [40].
- **Nondominated Sorting Genetic Algorithm II (NSGA-II):** A Pareto-based multi-objective evolutionary method jointly optimizes multiple indicators (e.g., energy efficiency, coverage, and fairness). It offers flexible trade-off exploration but requires post-processing/selection from the Pareto front, which can reduce interpretability for deployment compared with a single-objective criterion [41].

2.9. Implementation details and computational complexity

All simulations were implemented in Python and executed on a workstation equipped with an Intel Core 7 processor, 32 GB RAM, and an NVIDIA RTX 5050 GPU. The proposed ME-GA and all benchmark algorithms were evaluated under identical system configurations to ensure a fair comparison.

The computational complexity of ME-GA is primarily determined by the interaction between the evolutionary search process and the mission-level simulation used for fitness evaluation. At the outer level, the genetic algorithm operates over G generations with a population size of N_{pop}. In each generation, all candidate solutions (i.e., chromosomes) are evaluated using the mission-level simulator. Therefore, the overall time complexity can be estimated as

$$\mathcal{O}\left(G \cdot N_{\text{pop}} \cdot C_{\text{sim}}\right), \tag{15}$$

where C_{sim} denotes the computational cost of a single mission-level simulation.

The mission-level simulation is executed over a discrete time horizon consisting of T time slots. At each time step, the simulator updates the system state, including UAV positions, sensing status, buffer occupancy, energy consumption, and communication processes. These updates involve:

- UAV state updates, which scale linearly with the number of UAVs (M),
- PoI-related operations, including sensing progress and data demand updates, exhibit scalability in accordance with the number of PoIs (N), and
- communication and buffering operations, which are contingent upon active UAVs and their interaction with the BS.

Given that these operations are performed at every time slot, the simulation cost can be estimated as follows:

$$C_{\text{sim}} = \mathcal{O}(T \cdot (M + N)). \tag{16}$$

This finding suggests that the computational cost increases linearly with respect to the number of generations, population size, time horizon, number of UAVs, and number of PoIs.

Despite this complexity, the proposed approach remains computationally viable for moderate-scale scenarios. Furthermore, the fitness evaluation of chromosomes is independent and can be parallelized, thus offering the potential for substantial acceleration through the utilization of multi-core or GPU-based implementations.

In practice, the dominant computational cost arises from the mission-level simulation rather than the genetic operators, as crossover and mutation operations have relatively low complexity compared to time-stepped system updates. This characteristic has been observed in a number of simulation-based optimization frameworks and justifies the use of efficient simulation design and potential parallelization strategies

3. Results

This section evaluates the performance of the proposed ME-GA against five benchmark algorithms: Random, Greedy, MR-GA, EB-GA, and NSGA-II. All algorithms are subjected to testing under identical simulation settings utilizing a grid- and random-based Point of Interest (PoI) deployment with 100 PoIs and UAV fleet sizes ranging from 1 to 9. Each configuration was repeated over 10 independent runs with controlled random seeds to ensure statistical reliability.

The maximum fleet size of nine UAVs was selected to balance computational tractability and system complexity. Preliminary experiments indicated that beyond this range, performance improvements saturate while computational cost increases significantly.

In contrast to conventional formulations that rely on surrogate or multi-objective metrics, the proposed ME-GA directly optimizes mission-level energy efficiency, which is defined as the ratio between total delivered sensing data and total energy consumption. Consequently, all results are primarily analyzed with respect to this metric, with other performance indicators being utilized for interpretation and diagnostic analysis.

3.1. Mission-level energy efficiency

Mission-level energy efficiency, expressed in Byte per Joule (B/J), serves as the primary performance metric in this study. Fig. 3 depicts energy efficiency results across varying numbers of UAVs.

In both scenarios, the Greedy algorithm consistently attains the highest energy efficiency values; however, this apparent superiority must be interpreted with caution. Greedy attains high efficiency primarily by limiting both energy consumption and the amount of delivered data, resulting in a conservative operational strategy that does not fully exploit available UAV resources. Consequently, its high efficiency does not necessarily correspond to high mission productivity.

In contrast, the proposed ME-GA demonstrates consistently high and stable energy efficiency across all fleet sizes in both layouts. In the grid scenario, ME-GA exhibits efficiency in the range of approximately 260–285 B/J, with only a gradual decline observed as the number of UAVs increases. A similar trend is observed in the random layout, where efficiency decreases moderately from around 270 B/J to approximately 250 B/J as fleet size grows. This behavior is indicative of the increasing coordination complexity and communication overhead in larger UAV systems.

In comparison to other evolutionary baselines, ME-GA consistently outperforms NSGA-II, EB-GA, and MR-GA. Despite the fact that NSGA-II exhibits competitive performance at moderate fleet sizes (e.g., 3–4 UAVs), its efficiency significantly degrades as the number of UAVs increases, indicating limited scalability in handling larger mission configurations. EB-GA and MR-GA demonstrate relatively stable yet lower levels of efficiency, suggesting that enhancing energy balance or route structure alone is inadequate for achieving high mission-level efficiency.

The primary advantage of ME-GA is its capacity to balance energy consumption and data delivery. In contrast to Greedy, which attains efficiency through reduced activity, ME-GA maintains high efficiency while concurrently maintaining substantial data collection and delivery. This finding suggests that ME-GA is more effective in converting available energy into meaningful mission output.

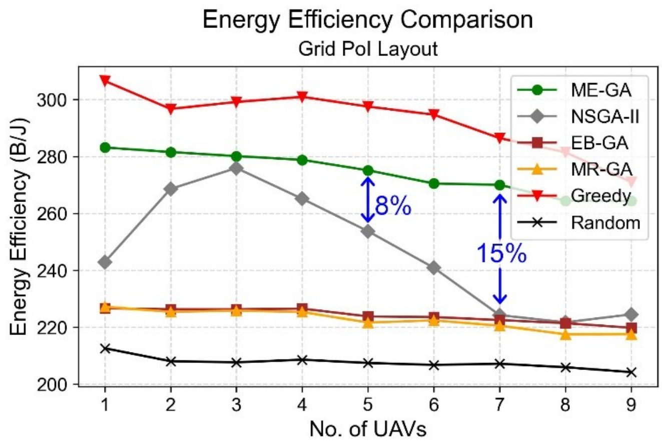

(a)

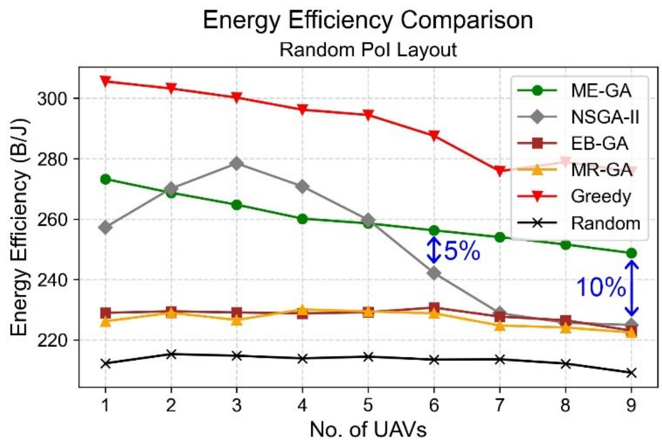

(b)

Fig. 3. Energy efficiency comparison: (a) grid PoI layout, and (b) random PoI layout

Furthermore, the consistency of ME-GA across both grid and random layouts demonstrates its robustness to spatial variations in PoI distribution. While all algorithms experience a certain degree of degradation in efficiency as the size of fleet increases, ME-GA exhibits a more controlled and predictable decline, thereby highlighting its capability to maintain performance under increasing system scale and complexity.

The finding of this study demonstrates that the direct optimization of mission-level energy efficiency enables ME-GA to achieve a favorable trade-off between energy expenditure and mission productivity. This, in turn, result in robust and scalable performance across a range of operational scenarios.

3.2. Task satisfaction and data delivery reliability

The task satisfaction ratio and the delivered data ratio offer complementary insights into the effectiveness with which each algorithm utilizes UAV resources to sense and transmit data. Across both spatial configurations, all algorithms demonstrate a consistent trend in which task satisfaction increases monotonically with the number of UAVs (Fig. 4).

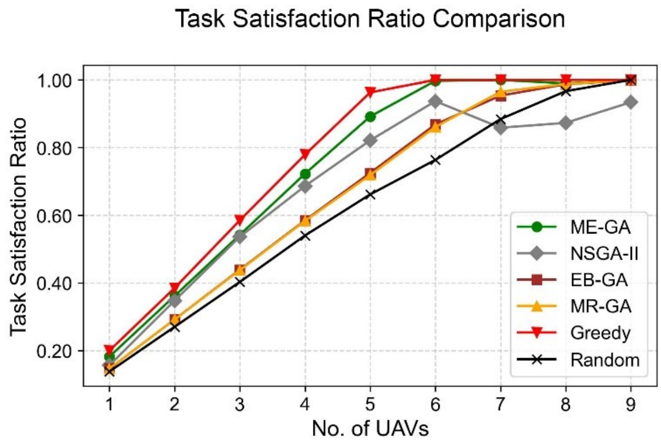

Fig. 4. Task satisfaction ratio comparison

This behavior is indicative of the anticipated enhancement in sensing capacity as additional UAVs are deployed. Greedy has been shown to achieve the fastest coverage growth, reaching near-complete coverage with fewer UAVs compared to other methods. ME-GA closely follows this precedent, achieving near-full coverage at moderate fleet sizes (approximately 5–6 UAVs), while maintaining a more balanced progression. It is evident that alternative evolutionary baselines, including NSGA-II, EB-GA, and MR-GA, demonstrate a more protracted convergence towards complete coverage. Moreover, Random exhibits persistent deficiency in terms of performance to its absence of structured coordination.

While Greedy is demonstrably superior in terms of task satisfaction, this advantage does not directly translate into effective mission performance. This phenomenon is clearly discernible upon examination of the delivered-data ratio. For small fleet sizes (1–5 UAVs), all algorithms achieve nearly perfect delivery (≈1.0), indicating that collected data can be reliably transmitted to the base station. However, as the number of UAVs increases beyond this range, noticeable divergence emerges.

Greedy experiences the most significant degradation in the delivered-data ratio at larger fleet sizes, despite achieving full coverage (Fig. 5). This finding suggests that the observed aggressive sensing behavior results in buffer accumulation and communication bottlenecks, thereby preventing efficient data transmission. A similar, though less pronounced, decline is observed in NSGA-II, EB-GA, and MR-GA, suggesting that these methods also struggle to maintain communication efficiency under increased system load.

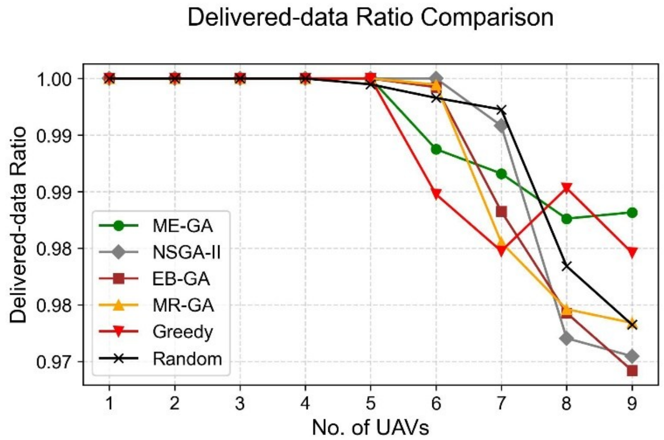

Fig. 5. Delivered-data ratio comparison

In contrast, ME-GA demonstrates a more regulated and incremental reduction in the ratio of delivered-data as the size of the fleet increases. While a slight decrease in performance is observed beyond 5–6 UAVs, the overall delivery performance remains consistently higher than most baseline methods. This finding suggests that ME-GA effectively balances sensing and communication processes, thereby preventing the accumulation of excessive data backlog while still maintaining high coverage.

The consistency of these trends across both grid and random layouts underscores a salient attribute of the proposed approach: the optimization of mission-level energy efficiency implicitly encourages a balanced allocation of sensing and communication resources. Consequently, ME-GA is capable of achieving near-complete coverage while maintaining reliable data delivery, even under increasing system complexity.

The findings of this study demonstrate that task satisfaction alone is insufficient to characterize mission performance. Algorithms such as Greedy have been demonstrated to facilitate rapid coverage expansion; however, this is often at the expense of delivery reliability. In contrast, ME-GA achieves a more desirable trade-off, ensuring that collected data is not only acquired but also successfully delivered, thereby improving the overall effectiveness of the mission.

3.3. Energy consumption and travel distance

It is imperative to consider total energy consumption and total travel distance as critical indicators of resource utilization efficiency. Across both spatial configurations, all algorithms demonstrate a consistent trend where total energy consumption and travel distance increase with the number of UAVs. This behavior is indicative of the elevated cumulative operational cost associated with the deployment of a greater number of UAVs, including propulsion, hovering, sensing, and communication activities. However, the rate of increase varies significantly across algorithms, revealing significant distinctions in terms of routing efficiency and mission coordination.

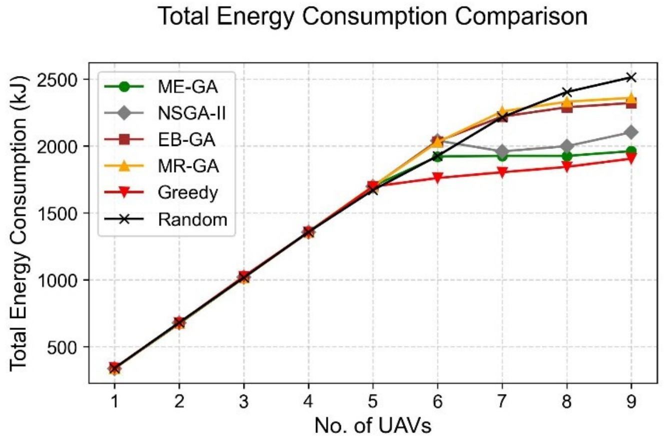

Fig. 6. Total energy consumption comparison

The proposed ME-GA model demonstrates a favorable and well-controlled growth pattern in both energy consumption and travel distance. While ME-GA does not always achieve the absolute minimum energy usage, it consistently maintains lower energy consumption than NSGA-II, EB-GA, MR-GA, and Random at larger fleet sizes (Fig. 6). It is noteworthy that beyond 5–6 UAVs, the discrepancy becomes more evident, suggesting that ME-GA effectively circumvents redundant movements and inefficient task allocation that commonly emerge in larger multi-UAV systems.

A similar pattern is observed in total travel distance (Fig. 7). It has been demonstrated that ME-GA generates significantly shorter routes in comparison to the majority of GA-based baselines, particularly at higher fleet sizes. In contrast, Random exhibits the maximum travel distance and energy consumption, indicative of its absence of coordination and inefficient exploratory behavior. NSGA-II, EB-GA, and MR-GA demonstrate moderate performance, yet their utilization still results in substantially elevated travel expenditures in comparison to ME-GA. This observation indicates that the optimization strategies employed by these algorithms do not sufficiently penalize excessive movement.

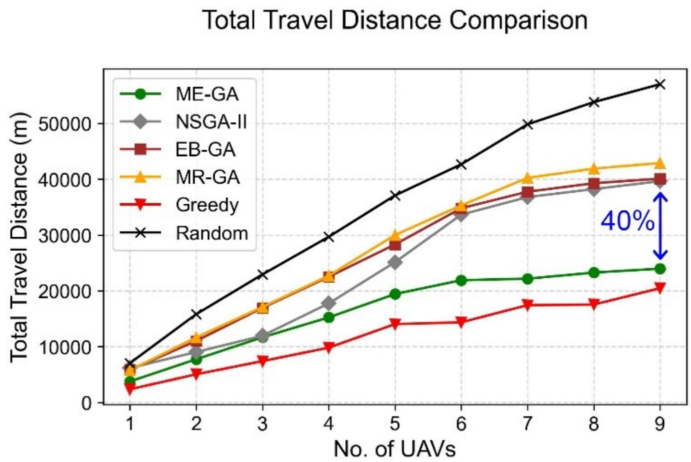

Fig. 7. Total travel distance comparison

Greedy consistently achieves the lowest energy consumption and shortest travel distance across all configurations. However, this apparent efficiency must be interpreted in the context of earlier findings. As demonstrated in Sections 3.2 and 3.3, Greedy accomplishes these cost reductions primarily by limiting its operational scope, resulting in reduced data delivery efficiency and degraded delivery reliability at larger fleet sizes. In essence, Greedy minimizes cost by reducing effort, rather than by enhancing efficiency.

3.4. Statistical analysis

To account for the stochastic nature of the evaluated algorithms, non-parametric statistical analysis was conducted utilizing the Wilcoxon signed-rank test. Paired samples were constructed by aligning the results of 10 independent runs for each UAV configuration, resulting in a total of 90 paired observations per comparison.

The statistical results for the primary metric, energy efficiency (measured in B/J), are outlined in Table 3. The proposed ME-GA significantly outperforms Random, MR-GA, EB-GA, and NSGA-II, with extremely small *p*-values ($p < 0.05$) and large effect sizes (Cliff's $\delta \geq 0.65$). These findings of this study suggest that the enhancement achieved by ME-GA are both statistically significant and practically meaningful.

In contrast, the comparison between ME-GA and Greedy does not yield a statistically significant difference ($p = 0.78$), with a negligible effect size ($\delta \approx 0.02$). This observation highlights a well-documented limitation of ratio-based metrics: Greedy attains comparable energy efficiency by concurrently diminishing both energy consumption and the volume of data transmitted.

Therefore, although Greedy may appear competitive when evaluated solely based on energy efficiency, it fails to deliver comparable mission-level performance when other operational metrics, such as coverage completeness and total delivered data, are considered. This underlines the significance of evaluating multi-UAV systems through the utilization of mission-oriented metrics beyond simple efficiency ratios.

The statistical analysis provides a robust validation of the ME-GA framework, demonstrating superiority across diverse mission scenarios.

Table 3. Statistical comparison of mission-level energy efficiency using Wilcoxon signed-rank test

Comparison	*p*-value	Cliff's δ	Effect	Interpretation
ME-GA vs. Random	$< 1 \times 10^{-10}$	0.94	Large	Statistically significant
ME-GA vs. MR-GA	$< 1 \times 10^{-8}$	0.79	Large	Statistically significant
ME-GA vs. EB-GA	$< 1 \times 10^{-8}$	0.82	Large	Statistically significant
ME-GA vs. NSGA-II	$< 1 \times 10^{-6}$	0.66	Large	Statistically significant
ME-GA vs. Greedy	0.78	0.02	Negligible	No significant difference

4. Discussion

The experimental results presented in Section 3 provide a comprehensive evaluation of the proposed ME-GA under varying fleet sizes and spatial configurations. This section employs a broader perspective to interpret these findings, focusing on the implications of optimizing mission-level energy efficiency as a single objective and its impact on system behavior. This behavior is consistent with prior studies on communication-constrained UAV systems, where increased sensing activity without coordination leads to congestion and reduced throughput [24,42].

4.1. Interpreting energy efficiency as a mission-level objective

As demonstrated in Section 3.1, it can be concluded that the Greedy algorithm is capable of attaining the highest energy efficiency values across most scenarios. However, this finding underscores a significant limitation of interpreting efficiency in isolation. Greedy attains high efficiency primarily by limiting both energy consumption and the amount of data delivered, effectively operating in a conservative regime where system activity is minimized.

Conversely, ME-GA exhibits a consistent capacity for high energy efficiency while concurrently sustaining significantly elevated levels of data collection and delivery. This finding suggests that ME-GA operates in a fundamentally different regime, wherein efficiency is attained through the effective resource utilization, rather than reduction of activity. From a mission-level perspective, this distinction is critical, as the ultimate objective is not merely to conserve energy, but to maximize the delivery of useful data per unit of energy.

This observation reinforces the validity of using mission-level energy efficiency as the optimization objective, as it encapsulate the trade-off between productivity and resource consumption in a single interpretable metric [43].

4.2. Emergent balance between coverage and communication

The findings presented in Section 3.2 demonstrate that ME-GA successfully attains near-complete coverage while maintaining high delivery ratios of data, despite the absence of explicit optimization of these metrics. This finding indicates that the proposed formulation induces an emergent balance between sensing and communication processes.

Conversely, Greedy expedites the attainment of comprehensive coverage; however, it exhibits a noticeable decline in delivery reliability at larger fleet sizes. This behavior suggests that aggressive sensing without coordination can result in communication bottlenecks, particularly when multiple UAVs attempt to transmit data concurrently [44].

In a similar vein, NSGA-II, EB-GA, and MR-GA demonstrate moderate performance in both coverage and delivery. However, these algorithms are unable to maintain a consistent balance as system complexity increases [45]. These observations underscore the fact that the explicit optimization of surrogate objectives, such as distance or load balancing, does not necessarily guarantee effective end-to-end mission performance.

The capacity of ME-GA to sustain both elevated coverage and reliable delivery suggests that optimizing energy efficiency implicitly regulates the interaction between sensing and communication, consequently leading to more coordinated system behavior.

4.3. Resource utilization and routing efficiency

As demonstrated in Section 3.3, an analysis of energy consumption and travel distance offers further insight into the operational characteristics of each algorithm. ME-GA demonstrates controlled growth in both metrics, indicating efficient routing and the avoidance of unnecessary movement.

Conversely, Random exhibits excessive travel distance and energy consumption, indicative of its absence of coordination. It is evident that NSGA-II, EB-GA, and MR-GA reduce this inefficiency to a certain extent. However, it should be noted that these methods still incur significantly higher costs than ME-GA, particularly at larger fleet sizes.

Greedy achieves the lowest energy consumption and travel distance, does so by limiting mission activity. This underscores a fundamental trade-off: the minimization of cost alone does not guarantee effective mission execution. Conversely, ME-GA model strives for a more balanced outcome by minimizing unnecessary movement while still ensuring the maintenance of high mission productivity.

These findings emphasize the importance of evaluating routing strategies within the context of mission-level objectives, rather than relying solely on local or surrogate optimization criteria.

4.4. Scalability and coordination complexity

The results presented in Section 3 demonstrate a consistent trend across all evaluated metrics as the number of UAVs increases. Whilst, the deployment of additional UAVs has been demonstrated to enhance sensing capacity and spatial coverage, it has also been shown to introduce increased coordination complexity, communication contention, and resource overhead [46].

A salient observation is the presence of diminishing returns more than moderate fleet sizes (typically around 5–6 UAVs). At this point, task satisfaction approaches a state of saturation, while the delivered-data ratio begins to degrade and total energy consumption continues to increase. This finding suggests that system performance is no longer constrained by sensing capability, but rather by coordination and communication efficiency.

It is evident that ME-GA demonstrates a more robust response to this increasing complexity. As demonstrated in Section 3, the proposed method maintains stable energy efficiency, controlled growth in energy consumption, and relatively high delivery reliability across all fleet sizes. This finding suggests that ME-GA implicitly adapts to coordination constraints by balancing sensing activity and communication load within the mission-level objective.

In contrast, Greedy exhibits a clear scalability limitation. While it performs well at small fleet sizes, its delivery performance degrades significantly at larger scales due to uncoordinated sensing behavior and communication bottlenecks. In a similar vein, NSGA-II, EB-GA, and MR-GA demonstrate moderate scalability; however, they are unable to maintain efficiency as system size increases, primarily due to the increase in travel distance and energy consumption without proportional gains in delivered data.

These observations highlight an important implication: the scalability of multi-UAV systems is not solely determined by the number of UAVs, but rather by the efficacy with which coordination complexity is managed. By directly optimizing mission-level energy efficiency, ME-GA implicitly regulates this complexity, thereby enabling more efficient resource utilization at larger scales.

4.5. Implication and limitations

The findings of this study have several practical implications. Firstly, it is demonstrated that a single-objective formulation based on mission-level energy efficiency can effectively capture complex trade-offs in multi-UAV systems. This approach has been shown to simplify the optimization problem while maintaining strong performance across multiple dimensions.

Secondly, the findings suggest that explicitly modeling mission dynamics, including sensing, buffering, and communication, is essential for attaining realistic and robust optimization outcomes.

However, it is important to note several limitations of this study. The present study is founded upon simulation under controlled conditions, including fixed UAV parameters and communication models. However, it is important to note that real-world deployments may introduce additional uncertainties, such as dynamic channel conditions, obstacles, and UAV failures.

Additionally, the computational expense of ME-GA exceeds remains that of simple heuristics, due to the need for repeated mission-level simulations. Whilst this cost is deemed manageable for the scenarios considered, further optimization or parallelization may be required for larger-scale applications.

5. Conclusion

This present study proposes a Mission-level Energy-aware Genetic Algorithm (ME-GA) for the optimization of multi-UAV data collection missions, with the objective being the direct maximization of mission-level energy efficiency, which is defined as the ratio of delivered data to total energy consumption. In contrast to conventional approaches that rely on surrogate or multi-objective formulations, the proposed method adopts a single-objective framework that integrates sensing, communication, and energy dynamics within a unified mission-level evaluation. The experimental results demonstrate that ME-GA achieves consistently high and stable energy efficiency across varying fleet sizes and spatial configurations, while maintaining high task satisfaction and reliable data delivery. In contrast to heuristic and conventional GA-based methods, ME-GA achieves a more balanced trade-off between resource consumption and mission output, avoiding both excessive exploration and overly conservative operation. These results confirm that mission-level energy efficiency serves as a physically meaningful and effective optimization objective for multi-UAV systems. Future work will extend the proposed framework to dynamic environments, heterogeneous UAV systems, and communication-aware coordination strategies.

References

1. M. Mozaffari, W. Saad, M. Bennis, Y.-H. Nam, and M. Debbah, *A Tutorial*

on UAVs for Wireless Networks: Applications, Challenges, and Open Problems, IEEE Commun. Surv. Tutor. 21 (2019) 2334–2360.

2. Y. Li, W. Chen, B. Fu, Z. Wu, and L. Hao, *A Global Coverage Path Planning Method for Multi-UAV Maritime Surveillance in Complex Obstacle Environments*, Drones. 8 (2024) 764.
3. M. Lyu, Y. Zhao, C. Huang, and H. Huang, *Unmanned Aerial Vehicles for Search and Rescue: A Survey*, Remote Sens. 15 (2023) 3266.
4. M. Tariq, A. Saadat, R. Ahmad, Z. Abaid, and J. J. P. C. Rodrigues, *Enhanced Border Surveillance Through a Hybrid Swarm Optimization Algorithm*, IEEE Sens. J. 23 (2023) 28172–28181.
5. M. H. Ridha, Y. F. Arifin, and A. S. Abdi, *Optimizing ground control points for UAV photogrammetry: a case study in slope stability mapping*, Commun. Sci. Technol. 10 (2025) 170–178.
6. A. Townsend, I. N. Jiya, C. Martinson, D. Bessarabov, and R. Gouws, *A comprehensive review of energy sources for unmanned aerial vehicles, their shortfalls and opportunities for improvements*, Heliyon. 6 (2020) e05285.
7. O. Cheikhrouhou and I. Khoufi, *A comprehensive survey on the Multiple Traveling Salesman Problem: Applications, approaches and taxonomy*, Comput. Sci. Rev. 40 (2021) 100369.
8. K. Bérczi, M. Mnich, and R. Vincze, *Approximations for many-visits multiple traveling salesman problems*, Omega. 116 (2023) 102816.
9. A. F. L. Villalba and E. C. G. L. Rotta, *Clustering and heuristics algorithm for the vehicle routing problem with time windows*, Int. J. Ind. Eng. Comput. 13 (2022) 165–184.
10. J. Chang, N. Dong, D. Li, W. H. Ip, and K. L. Yung, *Skeleton Extraction and Greedy-Algorithm-Based Path Planning and its Application in UAV Trajectory Tracking*, IEEE Trans. Aerosp. Electron. Syst. 58 (2022) 4953–4964.
11. Q. Meng, K. Chen, and Q. Qu, *PPSwarm: Multi-UAV Path Planning Based on Hybrid PSO in Complex Scenarios*, Drones. 8 (2024) 192.
12. J. Zheng, X. Sun, Y. Ji, and J. Wu, Research on UAV Path Planning Based on Improved ACO algorithm, 2023 IEEE 11th Joint International Information Technology and Artificial Intelligence Conference (ITAIC), Chongqing, China, 2023, pp. 762–770.
13. S. Zhang, W. Liu, and N. Ansari, *Joint Wireless Charging and Data Collection for UAV-Enabled Internet of Things Network*, IEEE Internet Things J. 9 (2022) 23852–23859.
14. B. Li, Q. Li, Y. Zeng, Y. Rong, and R. Zhang, *3D Trajectory Optimization for Energy-Efficient UAV Communication: A Control Design Perspective*, IEEE Trans. Wirel. Commun. 21 (2022) 4579–4593.
15. S. Fang and Z. Luo, Multi-Traveling Salesman Algorithm for UAV Swarms Based on Improved Genetic Algorithm, 2024 IEEE 6th International Conference on Power, Intelligent Computing and Systems (ICPICS), Shenyang, China, 2024, pp. 1027–1032.
16. S. Mahmoudinazlou and C. Kwon, *A hybrid genetic algorithm for the min–max Multiple Traveling Salesman Problem*, Comput. Oper. Res. 162 (2024) 106455.
17. X. Wu, Y. Yin, L. Xu, X. Wu, F. Meng, and R. Zhen, *MULTI-UAV Task Allocation Based on Improved Genetic Algorithm*, IEEE Access. 9 (2021) 100369–100379.
18. Y. He, K. Xiang, X. Cao, and M. Guizani, *Task Scheduling and Trajectory Optimization Based on Fairness and Communication Security for Multi-UAV-MEC System*, IEEE Internet Things J. 11 (2024) 30510–30523.
19. M. M. H. Rahman, M. Al-Naeem, A. Banerjee, and A. Sufian, *EETO-GA: Energy Efficient Trajectory Optimization of UAV-IoT Collaborative System Using Genetic Algorithm*, Appl. Sci. 13 (2023) 2535.
20. X. Huang, NSGA-II Algorithm in Path Planning of Multiple Unmanned Aerial Vehicle Collaborative Search Tasks, 2024 International Conference on Machine Intelligence and Digital Applications, Ningbo China, 2024, pp. 771–776.
21. Y. Yuan, H. Xu, and C. Tang, *Multi-Objective Emergency Path Planning Based on Improved Nondominant Sorting Genetic Algorithm*, Symmetry. 17 (2025) 1818.
22. H. Fu *et al.*, *Path Planning for Agricultural UAVs Based on Deep Reinforcement Learning and Energy Consumption Constraints*, Agriculture. 15 (2025) 943.
23. H. Zhang, A. Zhan, J. Han, C. Wu, and Z. Wang, *Integrated Path Planning, Spectrum and Power Allocation for Multi-UAV via Deep Reinforcement Learning*, IEICE Trans. Fundam. Electron. Commun. Comput. Sci. E108.A (2025) 856–860.
24. S. Xu, Z. Zhou, J. Li, L. Wang, X. Zhang, and H. Gao, *Communication-Constrained UAVs' Coverage Search Method in Uncertain Scenarios*, IEEE Sens. J. 24 (2024) 17092–17101.
25. H. Zhang, J. Luo, R. Li, M. Wei, X. Xie, and W. Wang, Adaptive Trajectory Optimization for UAV Swarms under Communication Constraints, 2025 IEEE International Conference on Unmanned Systems (ICUS), Changzhou, China, 2025, pp. 1751–1756.
26. A. Al-Hourani, S. Kandeepan, and A. Jamalipour, Modeling air-to-ground path loss for low altitude platforms in urban environments, 2014 IEEE Global Communications Conference, Austin, TX, USA, 2014, pp. 2898–2904.
27. A. Al-Hourani, S. Kandeepan, and S. Lardner, *Optimal LAP Altitude for Maximum Coverage*, IEEE Wirel. Commun. Lett. 3 (2014) 569–572.
28. V. Lala *et al.*, Channel Modelling for UAV Air-to-Ground Communication, 2024 5th International Conference on Emerging Trends in Electrical, Electronic and Communications Engineering (ELECOM), Balaclava, Mauritius, 2024, pp. 1–5.
29. *ETSI TS 138 214 - V15.9.0 - 5G; NR; Physical layer procedures for data (3GPP TS 38.214 version 15.9.0 Release 15)*, 2020.
30. S. Khan, M. Zeeshan, and Y. Ayaz, *Implementation and analysis of MultiCode MultiCarrier Code Division Multiple Access (MC–MC CDMA) in IEEE 802.11ah for UAV Swarm communication*, Phys. Commun. 42 (2020) 101159.
31. H. V. Abeywickrama, B. A. Jayawickrama, Y. He, and E. Dutkiewicz, *Comprehensive Energy Consumption Model for Unmanned Aerial Vehicles, Based on Empirical Studies of Battery Performance*, IEEE Access. 6 (2018) 58383–58394.
32. Y. Zeng, J. Xu, and R. Zhang, *Energy Minimization for Wireless Communication With Rotary-Wing UAV*, IEEE Trans. Wirel. Commun. 18 (2019) 2329–2345.
33. D. Datsko, F. Nekovar, R. Penicka, and M. Saska, *Energy-Aware Multi-UAV Coverage Mission Planning With Optimal Speed of Flight*, IEEE Robot. Autom. Lett. 9 (2024) 2893–2900.
34. Y. Wang, S. Fan, L. Wang, X. An, and D. Zhang, Research on Energy Efficiency Optimization and Path Planning for RIS-Assisted UAV Communication System, Proceedings of the 2024 3rd International Conference on Artificial Intelligence and Intelligent Information Processing, Tianjin China, 2024, pp. 217–222.
35. X. Dai, B. Duo, X. Yuan, and W. Tang, *Energy-Efficient UAV Communications: A Generalized Propulsion Energy Consumption Model*, IEEE Wirel. Commun. Lett. 11 (2022) 2150–2154.
36. DJI, DJI Mavic 4 Pro Specifications. Accessed: Dec. 20, 2025. [Online]. Available: https://www.dji.com/id/mavic-4-pro/specs.
37. R. Diankov and J. Kuffner, Randomized statistical path planning, 2007 IEEE/RSJ International Conference on Intelligent Robots and Systems, San Diego, CA, USA, 2007, pp. 1–6.
38. A. Vince, *A framework for the greedy algorithm*, Discrete Appl. Math. 121 (2002) 247–260.
39. Y. Cao, W. Wei, Y. Bai, and H. Qiao, *Multi-base multi-UAV cooperative*

reconnaissance path planning with genetic algorithm, Clust. Comput. 22 (2019) 5175–5184.

40. A. Shinde and R. Bichkar, Genetic Algorithm Based Energy Efficient and Load Balanced Clustering Approach for WSN, 2023 International Conference on Emerging Smart Computing and Informatics (ESCI), Pune, India, 2023, pp. 1–6.
41. K. Deb, A. Pratap, S. Agarwal, and T. Meyarivan, *A fast and elitist multiobjective genetic algorithm: NSGA-II*, IEEE Trans. Evol. Comput. 6 (2002) 182–197.
42. Y. Pan *et al.*, *Cooperative Trajectory Planning and Resource Allocation for UAV-Enabled Integrated Sensing and Communication Systems*, IEEE Trans. Veh. Technol. 73 (2024) 6502–6516.
43. O. Liubimov, I. Turkin, V. Cheranovskiy, and L. Volobuieva, *UAV Mission Computer Operation Mode Optimization Focusing on Computational Energy Efficiency and System Responsiveness*, Computation. 12 (2024) 235.
44. S. Alqefari and M. E. B. Menai, *Multi-UAV Task Assignment in Dynamic Environments: Current Trends and Future Directions*, Drones. 9 (2025) 75.
45. S. Sharma and V. Kumar, *A Comprehensive Review on Multi-objective Optimization Techniques: Past, Present and Future*, Arch. Comput. Methods Eng. 29 (2022) 5605–5633.
46. G. E. M. Abro, Z. A. Ali, and R. J. Masood, *Synergistic UAV Motion: A Comprehensive Review on Advancing Multi-Agent Coordination*, ICCK Trans. Sens. Commun. Control. 1 (2024) 72–88.